

## **STRUT-AND-TIE MODEL DESIGN PROVISIONS**

**Robin G. Tuchscherer, P.E., Ph. D.**, Datum Engineers Inc., Austin, Texas  
**David B. Birrcher, Ph. D.**, International Bridge Technologies, San Diego, California  
**Oguzhan Bayrak, Ph. D.**, University of Texas at Austin, Austin, Texas

### **ABSTRACT**

The overall objective of the research project summarized in this paper was to develop simple and safe design guidelines for deep beams. To accomplish the research objective and related tasks, a database of 868 deep beam tests was assembled from previous research. In addition, 37 beams were fabricated and tested with the following cross-sectional dimensions: 36"x48", 21"x75", 21"x42", and 21"x23". These tests represent some of the largest deep beam shear tests ever conducted. Based on an analysis of the database and the experimental program, the deep beam shear provisions in ACI 318-08 and AASHTO LRFD (2008) were found to be overly conservative. Thus, a new and simple strut-and-tie modeling (STM) procedure was proposed for the strength design of deep beam regions. The procedure is largely based on the *fib* (1999) design provisions. It is more accurate than the STM design method in ACI 318-08 and AASHTO LRFD (2008), yet just as conservative. With the use of the proposed provisions, the design of deep beams is more efficient and reliable. As a result, implementation of the new design provisions into AASHTO LRFD (2008) is recommended.

**Keywords:** Deep beam shear, strut-and-tie modeling, STM, triaxial confinement, efficiency factors

## INTRODUCTION

In this paper, the strut-and-tie design provisions recommended by the American Concrete Institute (ACI 318-08)<sup>1</sup>, the American Association of State Highway Transportation Officials (AASHTO LRFD, 2008)<sup>2-3</sup>, and The International Federation of Structural Concrete (*fib*, 1999)<sup>4</sup> are evaluated with a database of deep beam test results. Based on an analysis of these results, the provisions in AASHTO LRFD<sup>2</sup> and ACI 318<sup>1</sup> were found to be inefficient and overly conservative. As a result, a new design procedure was developed. The new design procedure is calibrated using only those test specimens that are the most representative of actual structures in the field, both in terms of their size and reinforcement details. The new design procedure is largely based on the design provisions recommended in *fib*<sup>4</sup>. Minor improvements to the *fib*<sup>4</sup> provisions are proposed in order to maintain consistency with ACI 318<sup>1</sup> and AASHTO LRFD<sup>2</sup>. When establishing the design procedure, consideration has been given to: simplicity; coordination with experimental data and theory; and coordination with standard design provisions.

## BACKGROUND

Typically, reinforced concrete members are designed to resist shear and flexural forces based on the assumption that strains vary linearly at a section. Referred to as the *Bernoulli hypothesis* or *beam theory*, the mechanical behavior of a beam is commonly determined by assuming that plane sections remain plane. The region of a structure where the Bernoulli hypothesis is valid is referred to as a B-region (B standing for *beam* or *Bernoulli*). In B-regions, the internal state of stress can be derived from the equilibrium of forces at a discrete cross-section. Therefore, the design of these regions is often referred to as a *sectional* design.

A *deep beam design* must be treated differently than a sectional design (or *slender beam design*) because the assumptions used to derive the sectional theory are no longer valid. In practice, engineers commonly encounter deep beams when designing transfer girders, pile supported foundations, shear walls, or corbels. In principal, a deep beam is a member whose shear span-to-depth ratio,  $a/d$ , is relatively small such that nonlinear shearing strains dominate the behavior. Nonlinear strain distributions are caused by abrupt changes in geometry or abrupt changes in loading. These regions of discontinuity are referred to as D-regions (D standing for *discontinuity* or *disturbance*). An elastic stress analysis suggests that the localized effect of a concentrated load or geometric discontinuity will attenuate about one member depth,  $d$ , away from a discontinuity (St. Venant's Principle). For this reason, D-regions are assumed to extend one member depth from the load or discontinuity. A deep beam is often comprised of both a concentrated load and support discontinuity. Therefore, nonlinear behavior can be expected if the load point is located less than twice the member depth,  $2d$ , from the support. Accordingly, MacGregor<sup>5</sup> defines a deep beam as follows:

*...a beam in which a significant amount of load is carried to the supports by a compression thrust joining the load and the reaction. This occurs if a concentrated load acts closer than about  $2d$  to the support, or for uniformly loaded beams with a span-to-depth ratio,  $l_n/d$ , less than about 4 to 5.*

A B-region and D-region is illustrated for an asymmetrically loaded simply supported beam in Fig. 1. The left side of the beam contains a B-region and stresses can be determined according to sectional methods. The right side contains a concentrated load located twice the member depth,  $d$ , from the support. Here, shear strains dominate the behavior and beam theory cannot be used to determine the internal state of stress.

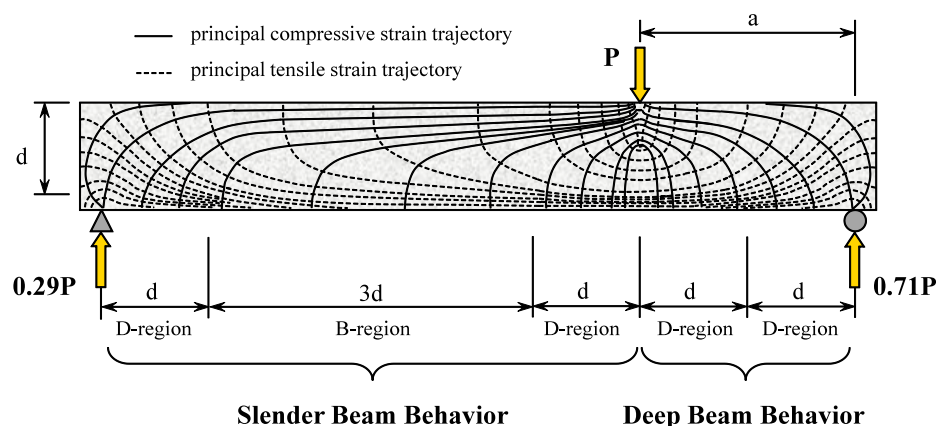


Fig. 1. Strain Distribution in Deep and Slender Portion of a Beam

ACI 318<sup>1</sup> and AASHTO LRFD<sup>2</sup> adopted strut-and-tie modeling for the design of deep beams or other regions of discontinuity in 2002 and 1994, respectively. A strut-and-tie model idealizes the complex flow of stresses in a structural member as axial elements in a truss member. Concrete *struts* resist the compressive stress fields and reinforcing steel *ties* resist the tensile stress fields. Struts and ties intersect at regions called *nodes*. Struts, ties, and nodes are the three elements that comprise a STM and they must be proportioned to resist the applied forces. According to the *lower bound theory of plasticity*, the capacity of a STM is always less than the actual capacity of the structure provided the following requirements are met: (i) the truss is in equilibrium, (ii) sufficient deformation capacity exists to distribute forces according to the assumed truss model, and (iii) the stresses applied to the elements do not exceed their yield or plastic flow capacity. If the yield capacity of an element is exceeded, the failure modes of a deep beam are the crushing of concrete in a strut or at the face of a node, yielding of a tie, or anchorage failure of a tie.

When designing a deep beam region using a strut-and-tie model, the first step is to determine the configuration of the truss model and the resulting forces in the critical elements. Two STMs for the beam depicted in Fig. 1 are provided in Fig. 2. In this paper, the first model is referred to as a single- or one-panel model; the second one is called a multiple- or two-panel model.

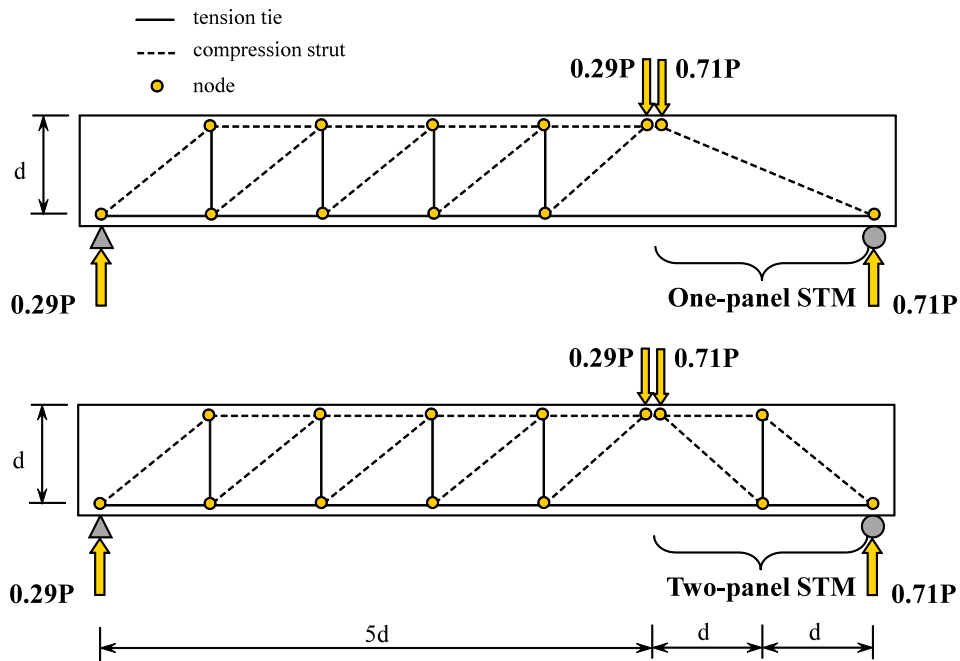


Fig. 2: One- and Two-Panel STM for Deep Beam

Either of the two models shown in Fig. 2 is acceptable provided that equilibrium and yield conditions are satisfied. The choice of the model is left to the discretion of the designer. However, if the orientation of the truss model varies significantly from the actual stress field, then the structure must undergo substantial deformation in order to develop the poorly assumed model. Thus, it is good practice for the STM to agree well with the dominant mechanism of force transfer in the structure.

Past researchers<sup>6-7</sup> agree that a direct-strut (one-panel model) is the predominant load carrying mechanism for structures with an  $a/d$  ratio less than 2.5 to 2. Also, experimental observations of this research<sup>8</sup> indicated that a direct strut was the primary load transfer mechanism for specimens with an  $a/d$  ratio of 1.85. Finally, the ACI 318<sup>1</sup> provisions allow a designer to use a single-panel strut when the  $a/d$  ratio is less than or equal to 2.1 (this is accomplished indirectly by limiting the strut angle to 25 degrees as  $\cot 25^\circ = 2.1$ ). Thus, it can be concluded that using a single-panel truss to represent a deep beam region is well founded based on experimental observations, past research, and current design provisions. For these reasons, a single-panel strut-and-tie model was used for the beams evaluated in this study.

### PROPORTIONING A STRUT-AND-TIE MODEL

After the selection of a strut-and-tie model, the next step of a STM design is to determine the geometry of the nodal regions. Defining the geometry of the nodal regions is required to calculate stresses on each nodal face. Subsequently, these stresses are compared to allowable design stresses. Generally, there are two techniques for proportioning nodes that have been established by previous researchers and code committees. The use of each technique results in hydrostatic or non-hydrostatic nodes. In both cases, nodal geometry is an idealization of regions in the strut-and-tie model where struts and ties are equilibrated. However, the resulting capacity of a truss model can be markedly different depending on the type of node. The influence that each of these node types has on a STM is illustrated in Fig. 3.

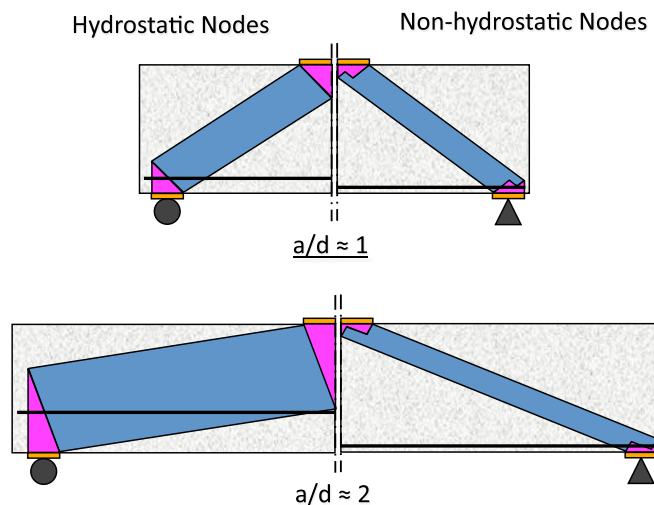


Fig. 3 Influence that Node Type has on Strut Proportions

As can be observed in Fig. 3, when the  $a/d$  ratio of a deep beam region increases, hydrostatic nodes can result in unrealistically large struts. Alternatively, strut widths resulting from non-hydrostatic nodal regions remain approximately constant as the  $a/d$  ratio increases.

Principal stresses are equal on all sides of a hydrostatic node. Therefore, the ratio of each nodal face is directly proportional to the force being applied to that face. However, as can be seen in Fig. 3, the nodal dimensions are often inconsistent with other beam details such as the location of the reinforcement and depth of the flexural-compression zone. Alternatively, the size of each face of a non-hydrostatic node is determined based on these aforementioned beam details. As a result, the stress applied to each face of a non-hydrostatic node is different. There is no requirement for equal stresses on all faces of a node.

The techniques used to proportion non-hydrostatic nodal regions have been well established by previous researchers and code provisions. In fact, these proportioning techniques are included in the current ACI 318<sup>1</sup> and AASHTO LRFD<sup>3</sup> STM provisions. Therefore, in order to maintain consistency with current design practice and code provisions, it is proposed that non-hydrostatic nodal regions be used to determine the critical stresses in a deep beam shear region.

It is important to note that the use of a consistent truss model is an essential requirement when evaluating code provisions. The critical nodal stresses are entirely dependent on the configuration of the model and geometry of the nodal regions. In this study, a single-panel strut-and-tie model was used to analyze deep beam test results and is illustrated in Fig. 4. Non-hydrostatic nodes were proportioned according to the techniques shown in Fig. 5.

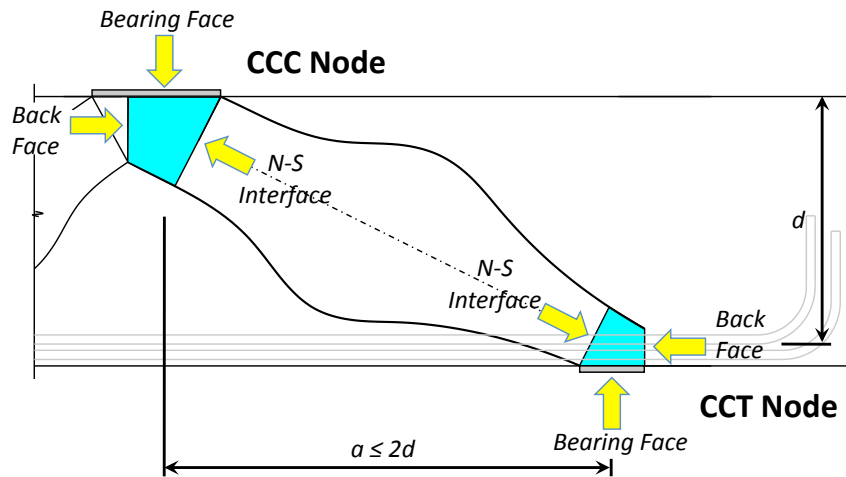


Fig. 4: Single panel strut-and-tie model with non-hydrostatic nodes

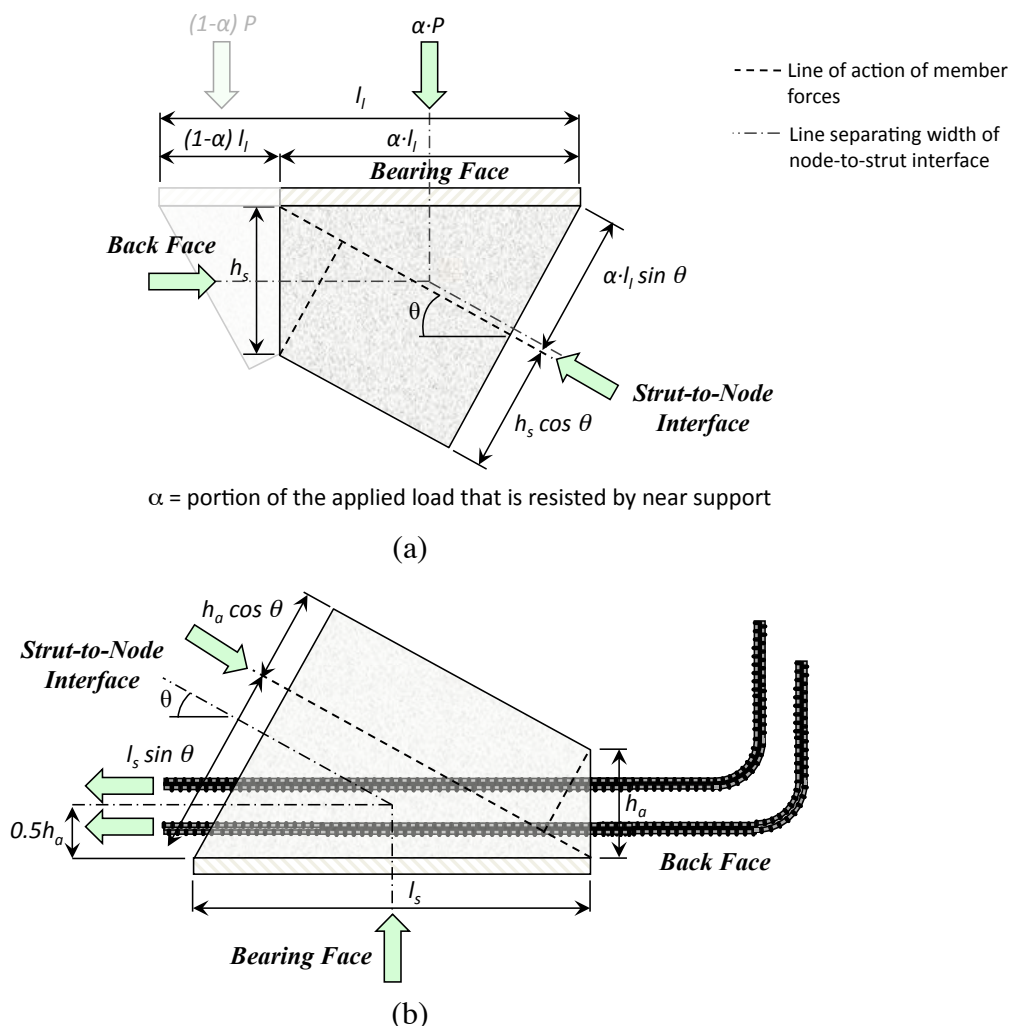


Fig. 5: Non-hydrostatic geometry of (a) CCC and (b) CCT node

Nodes are named based on the nature of the elements that frame into them. For example, the nodal zone where two struts and a tie intersect is referred to as a *CCT* node (*C* stands for *compression* and *T* stands for *tension*). If more than three forces intersect at a node, it is often

necessary to resolve some of the forces to end up with three resulting forces. In general, the CCC node occurs under an applied load. The size of the load plate,  $l_l$ , and portion of the load that is transferred to the near support is used to determine the area of the bearing face. Typically, the depth of the back face,  $h_s$ , is taken as the depth of the equivalent compressive stress block obtained from a typical flexural analysis. For a rectangular beam,  $h_s$  may be calculated according to Eq. 1.

$$h_s = \beta_1 c = \frac{(A_s f_s - A'_s f'_s)}{0.85 b_w d} \quad \text{Eq. 1}$$

Where:

- $A_s$  = Area of tension reinforcement, in<sup>2</sup>
- $A'_s$  = Area of compression reinforcement, in<sup>2</sup>
- $b_w$  = Web width, in.
- $f_s$  = Stress in tension reinforcement, psi
- $f'_s$  = Stress in compression reinforcement, psi

The bearing face of a CCT node,  $l_s$ , is determined based on the size of the bearing plate. The height of the back face,  $h_a$ , is taken as twice the distance from the near face of the beam to the centroid of the tension reinforcement.

## DEEP BEAM DATABASE

In order to evaluate deep beam shear provisions, a database containing 868 deep beam shear tests ( $a/d \leq 2.5$ ) was collected from previous literature. In addition to these 868 tests, 37 tests were conducted as part of the current research project<sup>8</sup>. The database containing all 905 tests is subsequently referred to as the *collection database*.

The collection database was filtered in two stages (Table 1). In the first stage, test results were removed due to a lack of adequate details necessary to perform a strut-and-tie analysis. The resulting database is referred to as the *filtered database*. In the second stage, additional test results were removed in which the specimens were considered less representative of members typically designed in practice. The resulting database is referred to as the *evaluation database*. An overview of the number of specimens that were removed from the database in each stage is provided in Table 1. Further explanation of the removal of these test results and a list of the references used to compile the collection database are provided elsewhere<sup>8</sup>.

Table 1. Filtering of the Deep Beam Database

<b>Collection Database</b>		<b>905 tests</b>
Stage 1 Filtering	• incomplete plate size information	- 284 tests
	• subjected to uniform loading	- 7 tests
	• stub column failure	- 3 tests
	• $f'_c < 2,000$ psi	- 4 tests
<b>Filtered Database</b>		<b>606 tests</b>
Stage 2 Filtering	• $b_w < 4.5$ in.	- 222 tests
	• $b_w d < 100$ in <sup>2</sup>	- 73 tests
	• $d < 12$ in.	- 13 tests
	• $\sum \rho_{\perp} < 0.001^*$	- 120 tests
<b>Evaluation Database</b>		<b>179 tests</b>

\* The summation of transverse reinforcement,  $\sum \rho_{\perp}$ , is defined in ACI 318-08<sup>1</sup>

It is the objective of the authors to only consider those beams that better represent actual deep beams designed in practice. Characteristics of the specimens in the evaluation database are illustrated in Fig. 6.

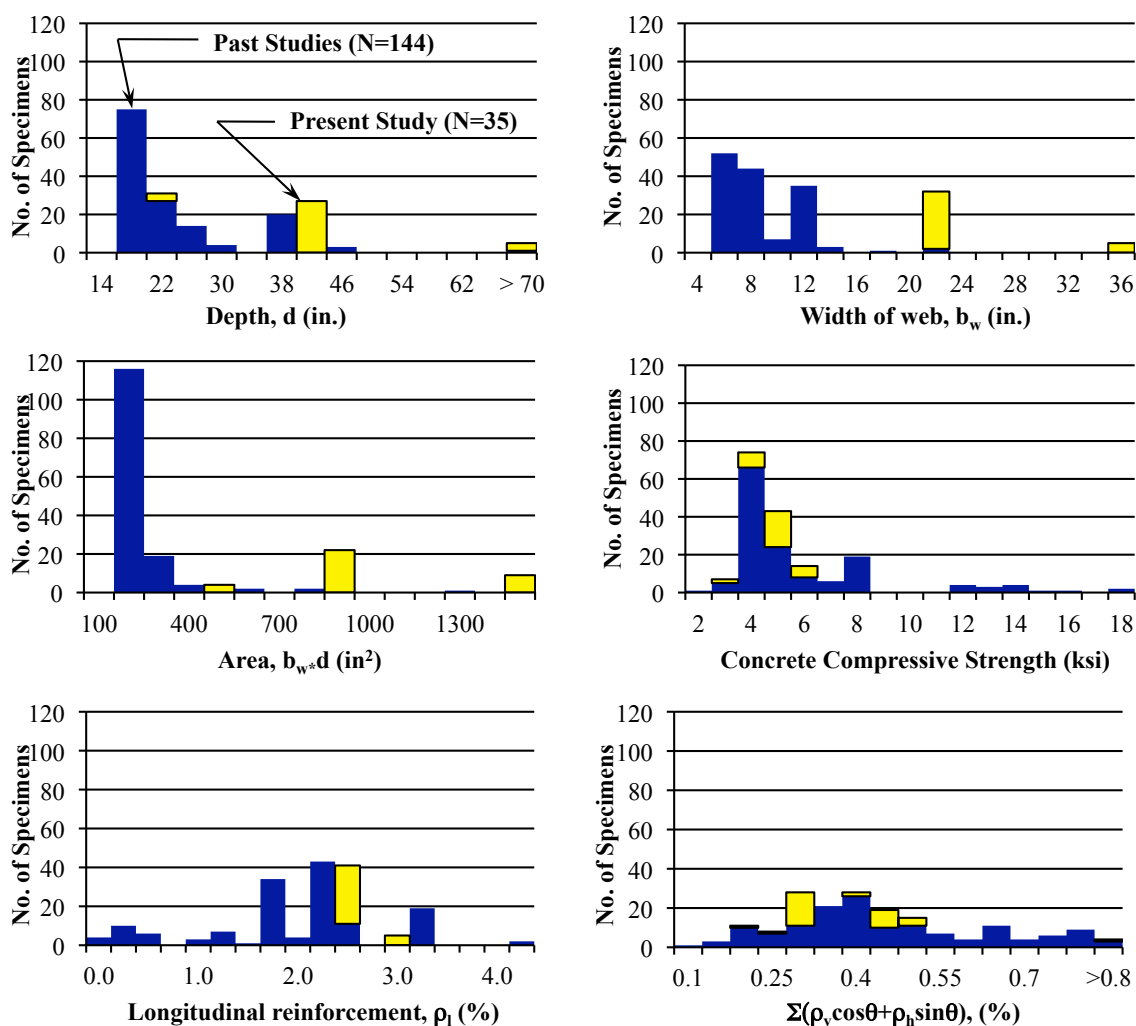


Fig. 6. Characteristics of the Test Specimens in the Evaluation Database

## EVALUATION OF CURRENT DESIGN PROVISIONS

In this section, the 179 test results in the evaluation database were used to evaluate the strut-and-tie design provisions in AASHTO LRFD<sup>2</sup>, ACI 318<sup>1</sup>, and *fib*<sup>4</sup>. The reported experimental capacity was compared to the strength calculated using the single-panel strut-and-tie model shown in Fig. 4 with each set of provisions. Based on the nodal geometries given in the model, the following seven stress checks were conducted for all of the beams in the database: 1) Back face of CCC and 2) CCT nodes; 3) Bearing face of CCC and 4) CCT nodes; 5) Node-to-strut interface at the CCC and 6) CCT nodes; and 7) stress in the tie reinforcement. The governing design check determined the calculated capacity of the specimen.

The aforementioned stress checks account for the possible failure modes of a deep beam or other D-region with two detailing exceptions. Proper anchorage of the tie must be provided to ensure that the tie reaches its design force. Similarly, minimum web reinforcement is required to provide a deep beam with sufficient deformation capacity to prevent premature splitting of the strut. All of the specimens in the database contained adequate anchorage and a minimum amount of web reinforcement to avoid these premature failure modes.

For reference, the allowable stress used from each set of STM provisions for the seven design checks is listed in Table 2. Additional information regarding each allowable stress can be found in the respective design specification.

Table 2. Summary of Stress Checks used to Evaluate Deep Beams

Element	Design Check	Design Provisions	Allowable Stress
CCC Node	Bearing	AASHTO LRFD	$0.85 f_c'$
		ACI 318	$0.85 f_c'$
		<i>fib</i>	$0.85 (1 - f_c'/40\text{ksi}) f_c'$
	Back Face	AASHTO LRFD	$0.85 f_c'$
		ACI 318	$0.85 f_c'$
		<i>fib</i>	$0.85 (1 - f_c'/40\text{ksi}) f_c'$
	Node to Strut Interface	AASHTO LRFD	$0.85 f_c'$
		ACI 318	$0.85 (0.75) f_c' = 0.64 f_c'$
		<i>fib</i>	$0.85 (1 - f_c'/40\text{ksi}) f_c'$
CCT Node	Bearing	AASHTO LRFD	$0.75 f_c'$
		ACI 318	$0.85 (0.80) f_c' = 0.68 f_c'$
		<i>fib</i>	$0.70 (1 - f_c'/40\text{ksi}) f_c'$
	Back Face	AASHTO LRFD	$0.75 f_c'$
		ACI 318	$0.85 (0.80) f_c' = 0.68 f_c'$
		<i>fib</i>	N/A
	Node to Strut Interface	AASHTO LRFD	$f_c' / (0.8 + 170\varepsilon_1) \leq 0.85 f_c' \dagger$
		ACI 318	$0.85 (0.75) f_c' = 0.64 f_c'$
		<i>fib</i>	$0.70 (1 - f_c'/40\text{ksi}) f_c'$
Tie	Tie	ALL	$f_y$

$\dagger \varepsilon_1$  is the principle tensile strain in cracked concrete<sup>2</sup>

The ratio of experimental to calculated capacity was determined for the beams in the evaluation database using the aforementioned design provisions and strut-and-tie model. A histogram of the findings is presented in Fig. 7.

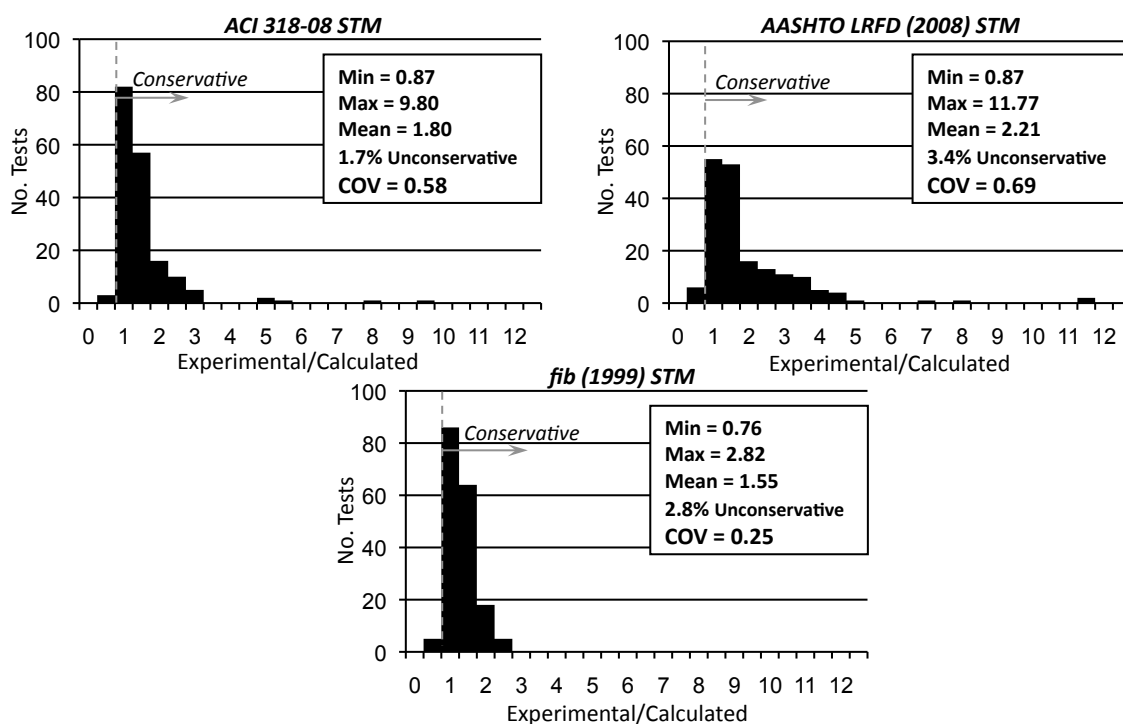


Fig. 7. Evaluation of STM Design Provisions (N=179)

When the experimentally determined capacity is greater than or equal to the calculated capacity (experimental/calculated  $> 1$ ), then the estimation of strength is a conservative prediction. Upon examination of the data in Fig. 7, it can be concluded that all three procedures provide adequately conservative estimates of strength. In all cases, less than 5% of the test data were unconservatively estimated. However, there was a considerable difference in the accuracy of each set of STM provisions as measured by the coefficient of variation (COV) and the mean ratio of experimental to calculated value. The implication of a high COV is an unnecessarily conservative estimate of strength. For example, the mean experimental/calculated ratio for the AASHTO LRFD<sup>2</sup> provisions (2.21) is 30% higher than it is for the *fib*<sup>4</sup> provisions (1.55). Therefore, on average, a beam designed according to AASHTO LRFD would have 30% less design capacity than the exact beam if it were designed according to *fib*<sup>4</sup>. In addition, at least one of the beams in the database carried an ultimate load almost twelve times greater than the AASHTO LRFD<sup>2</sup> design capacity (maximum experimental/calculated ratio = 11.77).

With a COV of 0.69 and a mean experimental/calculated value of 2.21, the STM procedure in AASHTO LRFD<sup>2</sup> was the least accurate design method. The reason can be attributed to the derivation of the method. The allowable stress at the CCT node-to-strut interface (Table 2) decreases as the  $a/d$  ratio increases. As the  $a/d$  ratio increases, the geometry of a non-hydrostatic node increases (Fig. 3). The combination of a decreasing allowable stress with non-hydrostatic node geometry will result in an overly conservative estimation of strength. It is likely that the AASHTO LRFD<sup>2</sup> provisions were originally derived with hydrostatic nodes. However, as noted previously, the use of hydrostatic nodes becomes impractical with

increasing  $a/d$  ratio. The use of non-hydrostatic nodes is more appropriate for design.

The  $fib^4$  method is considerably more accurate than the other two methods (COV of 0.25 for  $fib^4$  compared with 0.58 for ACI 318<sup>1</sup> and 0.69 for AASHTO LRFD<sup>2</sup>). The difference in accuracy can be attributed to the following:

- **Triaxial Confinement.**  $fib^4$  explicitly allows the allowable stress at all faces of a nodal zone to be increased when concrete surrounding the loaded area provides triaxial confinement.
- **Back Face of CCT Node.**  $fib^4$  does not consider bonding stresses at the back face of a CCT node to be critical – provided bars are anchored properly.
- **Efficiency Factors Vary with Concrete Strength.** The allowable stresses recommended by  $fib^4$  increase at a diminishing rate as the compressive strength of concrete increases.

It is the authors' goal to suggest improvements to the AASHTO LRFD<sup>2</sup> strut-and-tie model provisions. Based on the data presented in Fig. 7, it is clear that the  $fib^4$  procedure is the most accurate. According to MacGregor<sup>9</sup>, a STM design procedure should satisfy the following four criteria: (i) simplicity in application; (ii) compatibility with tests of D-regions; (iii) compatibility with other sections of the Code; (iv) and compatibility with other codes or design recommendations. With these considerations in mind, a proposed strut-and-tie design method was established that is largely based on the provisions in  $fib^4$ , but is compatible with other articles of AASHTO LRFD<sup>2</sup>.

## PROPOSED STRUT-AND-TIE DESIGN METHOD

The following method is recommended for strut-and-tie model design. It incorporates several features of the  $fib^4$  provisions, but is consistent with AASHTO LRFD<sup>2</sup> and ACI 318<sup>1</sup>.

The nominal strength of a nodal zone,  $F_n$ , shall be calculated as follows:

$$F_n = f_{ce} A_{nz} \quad \text{Eq. 2}$$

where,

$$\begin{aligned} f_{ce} &= \text{effective compressive strength of concrete in nodal zone, psi} \\ A_{nz} &= \text{cross-sectional area of the face of the nodal zone, in.}^2 \end{aligned}$$

The effective compressive strength,  $f_{ce}$ , on the face of a nodal zone shall be calculated as follows:

$$f_{ce} = m v f'_c \quad \text{Eq. 3}$$

where,

$m$  = triaxial confinement modification factor,  $\sqrt{A_2/A_1} \leq 2$  as defined in AASHTO LRFD<sup>2</sup>.

$v$  = node face efficiency factor taken as:

0.85 for bearing and back face of CCC nodes

0.70 for bearing and back face of CCT nodes

$0.45 \leq \left( 0.85 - \frac{f'_c}{20 \text{ksi}} \right) \leq 0.65$  for CCC and CCT node-to-strut interfaces with crack control reinforcement

0.45 for CCC and CCT node-to-strut interfaces without crack control reinforcement.

$f'_c$  = specified compressive strength of concrete, psi.

The triaxial confinement modification factor,  $m$ , is recognized in bearing calculations in AASHTO LRFD<sup>2</sup> and ACI 318<sup>1</sup>, but not in their respective STM provisions. It is well known that the strength and ductility of concrete is higher under triaxial compression than under uniaxial compression<sup>10</sup>. To confirm that triaxial confinement was applicable to deep beam tests, several specimens were tested in the current study<sup>8</sup> in which the dimensions of the bearing plates were the primary variable. The test results support the benefits of triaxial confinement of surrounding concrete for all faces of nodal regions. Thus, based on experimental data and while maintaining compatibility with bearing calculations in AASHTO LRFD<sup>2</sup> and ACI 318<sup>1</sup>, the same modification factor is recommended in the proposed STM provisions.

The node face efficiency factor,  $v$ , is similar to that in AASHTO LRFD<sup>2</sup> and ACI 318<sup>1</sup> for the bearing face at CCC and CCT nodes and for the back face of CCC nodes. However, for the back face of CCT nodes, bond stresses from an adequately developed tension tie (Fig. 8a) are not applied to the back face of the node. Based on the experimental results of this testing program<sup>8</sup>, recommendations of *fib*<sup>4</sup>, recommendations of past researchers<sup>11-12</sup>, and an analysis of the database<sup>8</sup>, it was determined that it is unnecessary to apply the bonding stresses from a developed bar to the back face of a CCT node. Therefore, in accordance with the recommendations of *fib*<sup>4</sup>, only directly applied stresses such as those due to bearing of a plate or due to an external indeterminacy (Fig. 8b and c) are applied to the back face of CCT nodes and checked with the 0.70 efficiency factor.

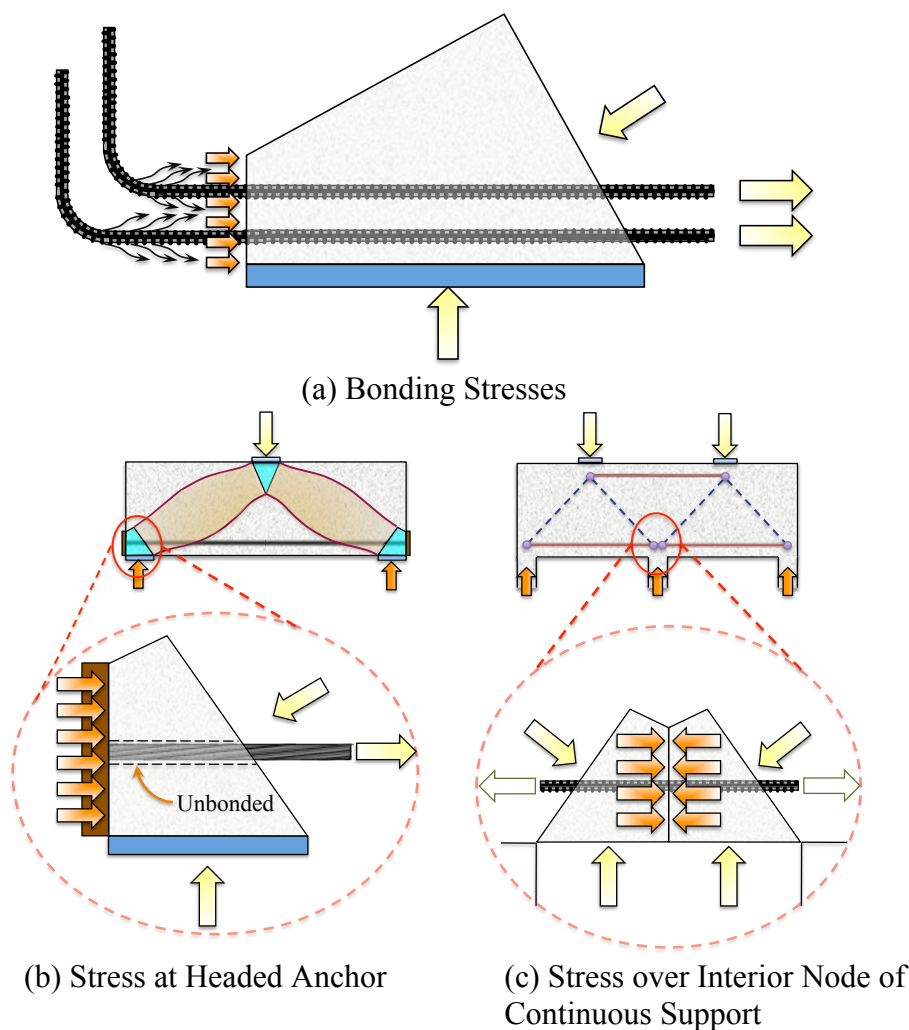


Fig. 8. Stress Conditions at the Back Face of a CCT Node.

In the proposed STM provisions (Eq. 3), the efficiency factor at the node-to-strut interface varies with the compressive strength of concrete and has a minimum and maximum limit of 0.45 and 0.65, respectively. Premature strut splitting is avoided by providing orthogonal grids of web reinforcement or by limiting the efficiency factor at the node-to-strut interface to 0.45.

No concrete stress checks are required in the proposed provisions (Eq. 3) in CTT or other similarly *smear*d nodal regions. Smear'd nodes refer to those regions that are not bounded by a bearing plate. Forces from compressive struts spread – or smear – and are equilibrated by multiple stirrups or ties. According to Schlaich et al.<sup>13</sup>, the geometry of smear'd nodes is not discrete, and therefore, checking stress limits is unnecessary. Tension reinforcement in CTT nodes near reentrant corners or voids should be well distributed in order to reduce high stress concentrations<sup>4</sup>, and ties in CTT nodes must be adequately developed or anchored.

In summary, the recommendations outlined by *fib*<sup>4</sup> were used to formulate a new STM design procedure. The following attributes of the proposed STM design procedure are consistent with the *fib*<sup>4</sup> provisions:

- Disregard the stress check at the back face of the CCT node when the applied force is the resultant of bonding stresses from a sufficiently anchored tie.

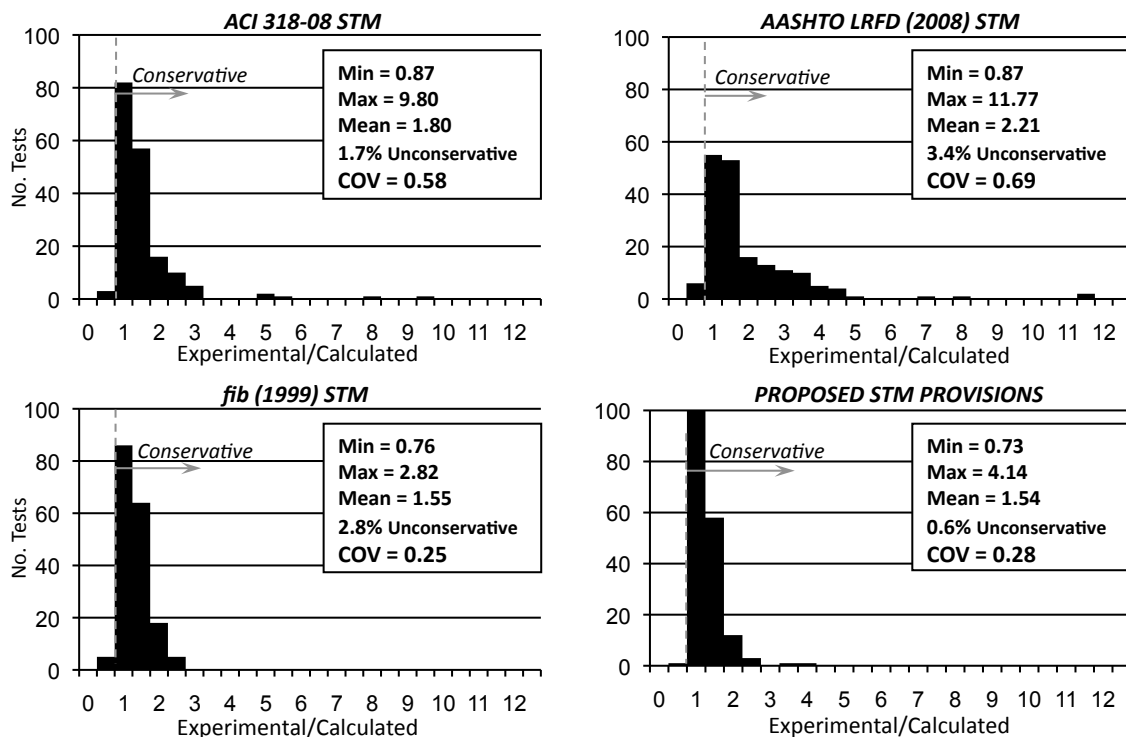
- Increase the allowable stress in triaxially confined nodal regions.
- At the CCC and CCT strut-to-node interface, the efficiency of concrete decreases as the compressive strength increases.

The following attributes of the proposed STM provisions are consistent with the ACI 318<sup>1</sup> and AASHTO LRFD<sup>2</sup> provisions:

- A triaxial confinement modification factor is used to account for the increase in nodal capacity due triaxial confinement. The modification factor is expressed the same as for bearing capacity.
- In accordance with ACI 318<sup>1</sup>, the efficiency of the CCC and CCT node-to-strut interfaces are identical.
- At the bearing and back face of the CCC node, the efficiency of concrete is a constant value of 0.85.
- At the bearing face of the CCT node, the efficiency of concrete is a constant value of 0.70.

### **ASSESSMENT OF THE PROPOSED STRUT-AND-TIE DESIGN METHOD**

An assessment of the proposed method is presented in Fig. 9. The ratio of experimental to calculated shear capacity is determined for the beams in the evaluation database and presented in the same manner as previously shown (Fig. 7). As can be observed, the proposed strut-and-tie modeling procedure is a significant improvement over the current ACI 318<sup>1</sup> and AASHTO LRFD<sup>2</sup> procedures. As may be expected, the proposed procedure is similarly accurate and conservative as the *fib*<sup>4</sup> provisions. As it is, the proposed provisions are calibrated in order to maintain consistency with ACI 318<sup>1</sup> and AASHTO LRFD<sup>2</sup>.



*In accordance with ACI 318-08 and AASHTO LRFD (2008), the proposed method contains a limit on the triaxial confinement modification factor equal to 2; whereas, fib<sup>4</sup> limits this factor to 4. The proposed method would perform better if the limit were increased to 4 [Mean = 1.51, 0.6% unconservative, COV = 0.22].*

Fig. 9. Evaluation of STM Design Provisions: Evaluation Database (N=179)

The specimens in the evaluation database were selected because they more accurately represent beams designed in practice both in terms of their size and reinforcement details. The criteria used to select these test specimens were determined by the authors and are listed in Table 1. It is also of interest to evaluate the performance of the proposed provisions for a dataset other than that which was used to calibrate the proposed procedure. Accordingly, the proposed STM provisions are compared with the ACI 318<sup>1</sup>, AASHTO LRFD<sup>2</sup>, and fib<sup>4</sup> provisions for all of the beams in the filtered database that contain a minimum amount of transverse reinforcement (Fig. 10).

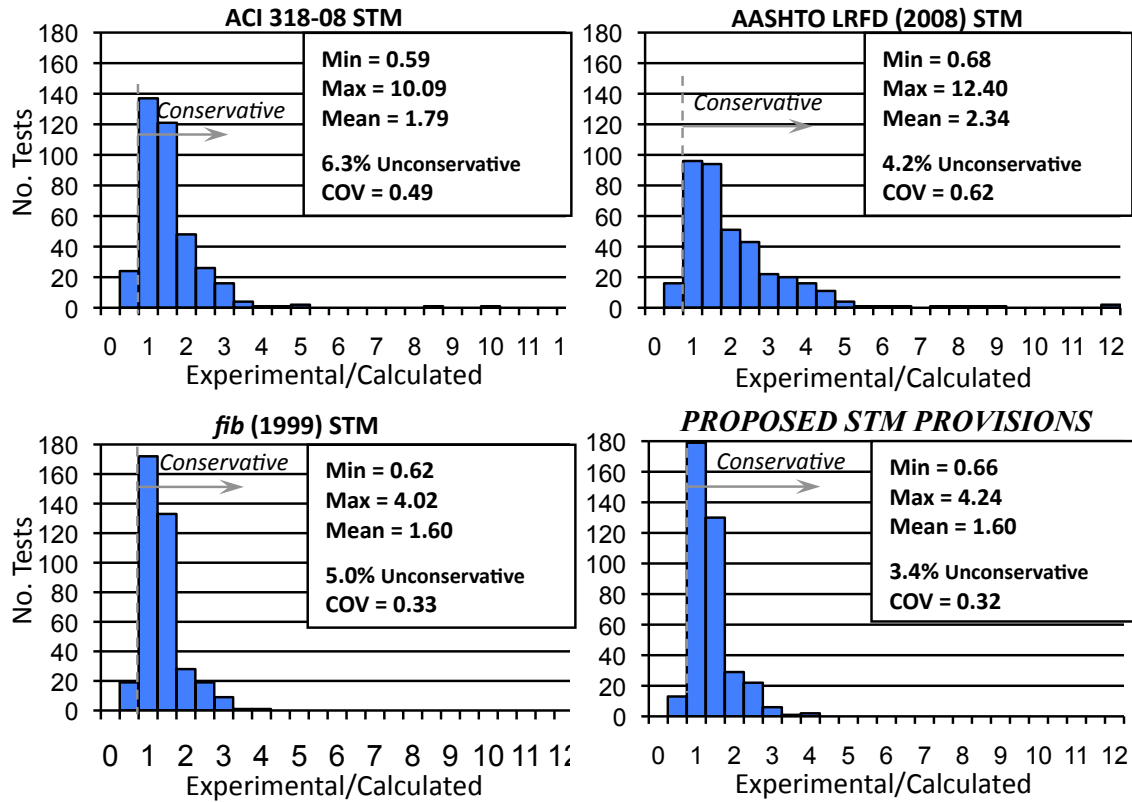


Fig. 10. Evaluation of STM Design Provisions: Filtered Database with  $\rho_1 > 0.1\%$  (N=382)

The tests evaluated in Fig. 10 constitute every deep beam shear test that could be found in the literature provided the test contained adequate bearing plate information and a minimal amount of transverse reinforcement. Although many of the beams in the filtered database were not used to calibrate the authors' recommendations, it can still be observed that the proposed STM procedure is a significant improvement over the ACI 318<sup>1</sup> and AASHTO LRFD<sup>2</sup> provisions.

## SUMMARY AND CONCLUSION

A new STM design procedure was developed for the design of deep beams. The new method was formulated based on the methodology used in *fib*<sup>4</sup> while maintaining consistency with ACI 318<sup>1</sup> and AASHTO LRFD<sup>2</sup>. In addition, the proposed method was calibrated based on beams that were considered to best represent actual structures. Thus, it can be concluded that the proposed design method maintains consistency with current provisions and established principles of STM. Based on the results of this study, it is strongly believed that the proposed STM method is valid for other types of structures.

In developing an STM procedure, it was necessary to explicitly define the truss geometries. This step cannot be over-emphasized as the performance of an STM methodology and its efficiency factors are intrinsically linked to the geometry of the nodal regions. Thus, the proposed STM provisions are based on an explicitly defined single-panel truss model with non-hydrostatic nodes. This single-panel model may be used as a basis for determining the configuration of forces in most deep beam regions.

Another important aspect of the new STM design methodology is that it was comprehensively derived based on all the stress checks that constitute an STM design. Stress checks at all six nodal faces (three faces at CCC and three faces at CCT nodes) and in the longitudinal tie were performed for all of the beams in the evaluation database. The splitting of the strut was indirectly accounted for by only considering those beams that contained a minimum amount of transverse reinforcement. Thus, the newly proposed design procedure considers every facet of an STM design. Accordingly, the following conclusion is made:

*The newly proposed STM procedure is: (i) simpler; (ii) more accurate and (iii) as safe as the ACI 318-08 and AASHTO LRFD (2008) STM design provisions. The procedure is based on established principles of strut-and-tie design, on tests of D-regions, and on the procedures in ACI 318-08, AASHTO LRFD (2008), and fib (1999) STM provisions. Finally, the procedure is practical and has been derived in a comprehensive and transparent manner.*

## **ACKNOWLEDGEMENTS**

The authors are sincerely grateful to the Texas Department of Transportation (TxDOT) for providing the funds to conduct this research study. The recommendations of the project director Dean Van Landuyt (Bridge Division) and other members of TxDOT including John Vogel (Houston District) and David Hohmann (Bridge Division) are deeply appreciated.

The authors would like to thank Matt Huizinga for his technical contributions and assistance with the experimental portion of the project. Also, the recommendations of Dr. James Jirsa, Dr. Sharon Wood, and Dr. John Breen improved the quality of this research and are greatly valued.

**REFERENCES**

1. ACI Committee 318-08, *Building Code Requirements for Reinforced Concrete (ACI 318-08)*, American Concrete Institute, Farmington Hills, MI, 2008, 465 pp.
2. AASHTO LRFD, *2008 Interim Revisions, Bridge Design Specifications, 4th Edition, 2007*, American Association of State Highway and Transportation Officials, Washington, D.C., 2008, 660 pp.
3. AASHTO, *Standard Specifications for Highway Bridges, 17<sup>th</sup> Edition*, American Association of State Highway and Transportation Officials, Washington, D. C., 2002, 1520 pp.
4. *fib* Recommendations, *Structural Concrete, Textbook on Behaviour, Design, and Performance*, Volume 3, International Federation for Structural Concrete, Lausanne, Switzerland, 1999, 269 pp.
5. MacGregor, J. G., *Reinforced Concrete, Mechanics and Design*, 3rd Edition, Prentice Hall, New Jersey, 1997, 939 pp.
6. Collins, M.P. and Mitchell, D., *Prestressed Concrete Structures*, Response Publications, Toronto and Montreal, 1997.
7. Kani, M. W.; Huggins, M. W.; and Wittkopp, R. R. (edited by), *Kani on Shear in Reinforced Concrete*, University of Toronto Press, Toronto, 1979, 225 pp.
8. Birrcher, D. B.; Tuchscherer, R. G.; Huizinga, M. R.; Bayrak, O.; Wood, S. L.; Jirsa, J. O.; Strength and Serviceability Design of Reinforced Concrete Deep Beams, Report No. 0-5253-1, Center for Transportation Research, University of Texas at Austin, Austin, TX, April 2009, 376 pp.
9. MacGregor, J. G., "Derivation of Strut and Tie Models for the 2002 ACI Code," *ACI SP-208 Examples for the Design of Structural Concrete with Strut-and-Tie Models*, American Concrete Institute, Michigan, 2002, 242 pp.
10. MacGregor, J. G. and Wight, J. K., *Reinforced Concrete, Mechanics and Design*, 4<sup>th</sup> Edition, Pearson Prentice Hall, New Jersey, 2005, 1132 pp.
11. Thompson, M. K.; Young, M. J.; Jirsa, J. O., Breen, J. E., and Klingner, R. E., *Anchorage of Headed Reinforcement in CCT Nodes*, Research Report 1855-2, Center for Transportation Research, University of Texas at Austin, Austin, Texas, 2003.
12. Brown, M. D.; Sankovich, C. L.; Bayrak, O.; Jirsa, J. O.; Breen, J. E.; and Wood, S. L., *Design for Shear in Reinforced Concrete Using Strut-and-Tie Models*, Report No. 0-4371-2, Center for Transportation Research, University of Texas at Austin, Austin, Texas, Apr. 2006.
13. Schlaich, J., Schäfer, K. and Jennewein, M., "Toward a Consistent Design of Structural Concrete," *PCI Journal*, Vol. 32, No. 3, May-June 1987, pp.74-150.